An Adaptive First-Order Polarization-Mode Dispersion Compensation System Aided by Polarization Scrambling: Theory and Demonstration

Hok Yong Pua, Kumar Peddanarappagari, Benyuan Zhu, Christopher Allen, Kenneth Demarest, and Rongqing Hui

***Abstract*—An adaptive polarization-mode dispersion (PMD) compensation system has been developed to cancel the effects of first-order PMD by producing a complementary PMD vector in the receiver. Control parameters for the PMD compensation system comprised of a polarization controller and a PMD emulator are derived from the nonreturn-to-zero (NRZ) signal in the channel to be compensated. Estimates of the link's differential group delay (DGD) and principal states of polarization (PSP's) based on this signal are reliable when the signal power is equally split between the link's two PSP's; however this condition cannot be assumed. To meet this requirement, we scramble the state of polarization (SOP) of the input signal at a rate much greater than the response time of the PMD monitor signal so that each sample represents many different SOP alignments. This approach allows the effective cancellation of the first-order PMD effects within an optical fiber channel.**

***Index Terms*—Compensation equalizers, optical fiber communication, optical polarization-mode dispersion, polarization scrambling.**

I. Introduction

DISPERSION in optical fiber communication systems degrades the optical channel signal quality by distorting signal waveforms. In digital systems dispersion can produce intersymbol interference (ISI). As the signal bandwidth is increased, the effects of dispersion become more significant. If not dealt with, dispersion represents a barrier to increasing the channel capacity. Effective techniques have been developed either to avoid or compensate for the dominant dispersion phenomena (e.g., modal, waveguide, and chromatic). However, among the dispersive phenomena in optical fiber, the effect of polarization-mode dispersion (PMD) is particularly difficult to compensate as its characteristics vary temporally. Fluctuating environmental factors (such as temperature, wind, and atmospheric pressure) can change the characteristics of PMD and hence its impact on optical channel quality.

The birefringence of optical fiber supports two degenerate modes, each having different propagation velocities, giving rise to PMD. To gain a better understanding of PMD, models have been developed that successfully predict the statistically observed effects in fiber. In these models, a long fiber link is modeled as a concatenated series of linearly birefringent, optical-fiber segments, each having a fixed birefringence, a fixed segment length corresponding to the fiber's random mode coupling characteristic length (L_h). The orientation of the principle axes from one segment to the next is treated as a random variable [1]. At every junction between segments, the energy from each incident pulse is split into two orthogonally polarized pulses, representing the mode coupling that occurs in fiber due to perturbations in local birefringence. After several such perturbations, the original pulse becomes a large ensemble of small pulses, dispersed in time. For the special case of a system using a light source whose coherence time is greater than the PMD-induced delays and a fiber whose optical loss is polarization independent, the PMD phenomenon in a long fiber link behaves in accordance with a high-coherence model, which incorporates the concept of principal states of polarization (PSP's). This means that, over a limited bandwidth, the link will behave as a randomly birefringent optical fiber such that an input optical pulse whose state of polarization (SOP) is aligned with one of the link's two input PSP's will emerge from the fiber's far end as a single pulse, unchanged in shape and polarized along the fiber's corresponding output PSP. From this model, we know that an input pulse aligned with neither input PSP will emerge as two orthogonally polarized pulses, separated in time by the link's differential group delay (DGD).

This model is frequency independent and valid to first order only. For wider bandwidths higher order effects must be considered resulting in frequency dependent polarization and dispersion [1], [2]. The bandwidth over which the PSP's can be assumed constant depend on the properties of the fiber and has been shown to vary inversely with the mean differential group delay (DGD) [3]. While the minimum bandwidth of the PSP's in single-mode fibers was found to be always over 50 GHz [3], this bandwidth for standard single-mode fiber is of the order of 100 GHz [1].

Time-varying environmental factors can change the mechanical stress on the fiber, causing localized changes in the birefringence characteristics of the fiber. This, in turn, affects the orientation of the PSP's and the DGD of the fiber link. For an optical transmitter with a fixed SOP, as the link's input PSP's change orientation, the relative intensities of the two orthogonal pulses will vary, and, at times, all of the energy will appear in only one pulse (resulting in no discernable PMD effects).

For long fiber links (lengths $\gg L_h$), the mean PMD increases with the square root of the link length.For example, in standard single-mode fiber, the typical random mode coupling characteristic length (L_h) is 100 m and the PMD is typically

Manuscript received October 25, 1999; revised February 23, 2000.

The authors are with the Lightwave Communication Systems Laboratory, University of Kansas, Lawrence KS 66045 USA.

Publisher Item Identifier S 0733-8724(00)05079-9.

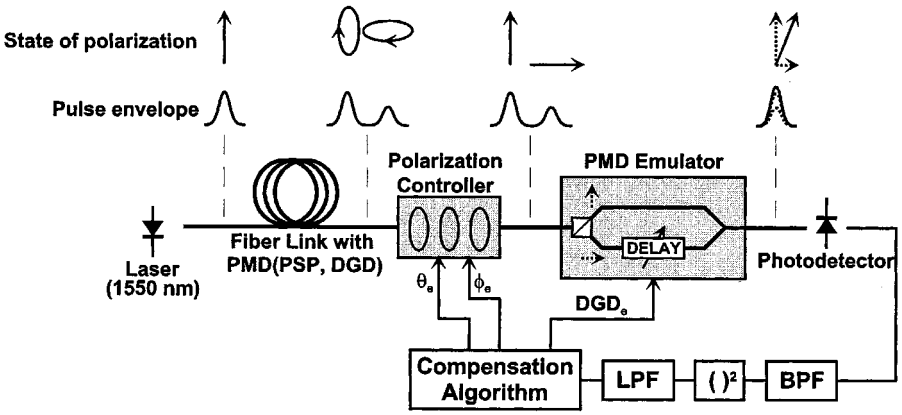

Fig. 1. Functional block diagram illustrating the adaptive PMD compensation system showing the evolution of the envelope and state of polarization for a single transmitted pulse as it progresses from the transmitter through the link, after the polarization controller, and as it emerges from the PMD emulator. BPF: bandpass filter; $(\,)^2$: square-law detector; LPF: low-pass filter.

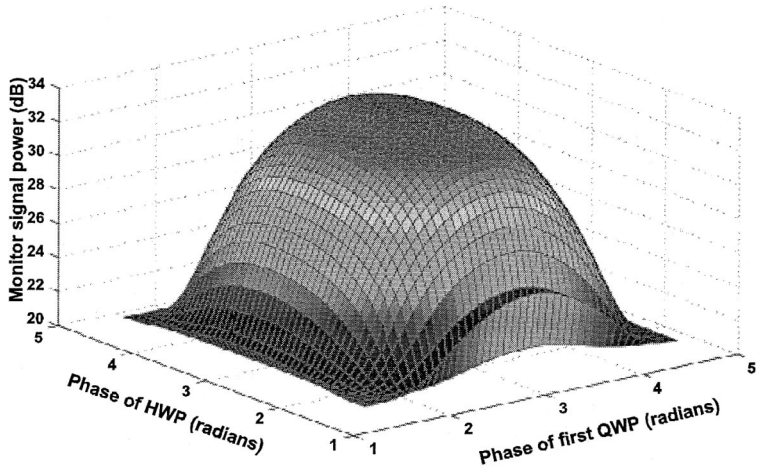

Fig. 2. Example of a simulated transfer function of monitor signal power versus polarization controller settings. The input signal power is assumed to be equally split on the two input PSP's and the DGD in both the link and the PMD emulator is 50 ps.

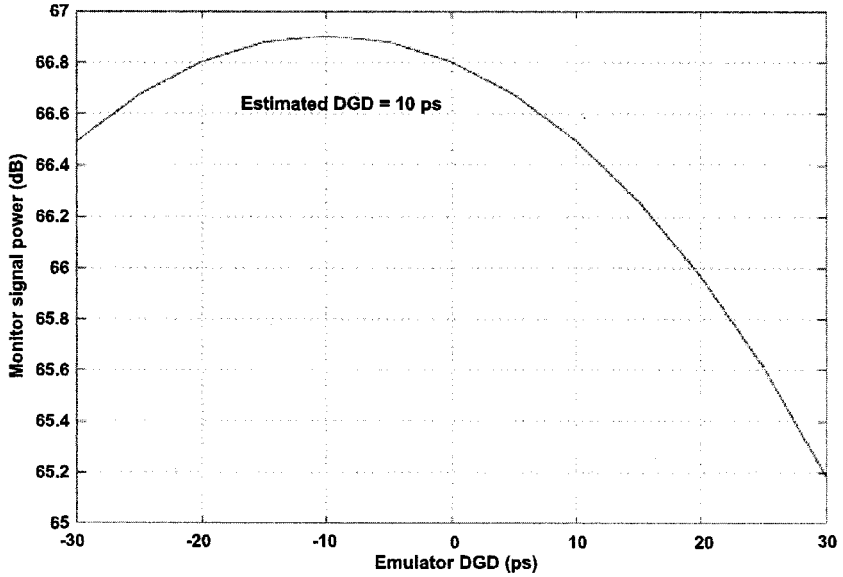

Fig. 3. Simulated transfer function relating the monitor signal power versus emulator DGD that is used to estimate the link DGD. For this case the link DGD is 10 ps and the signal power is equally split on the input PSP's.

0.1 ps/(km)$^{1/2}$ [1]. Therefore, for a typical terrestrial fiber link length of 500 km, the mean anticipated PMD would be 2.24 ps. This level of PMD is generally insignificant for channel data rates of 2.5 Gb/s or less, but would certainly be significant for data rates of 10 Gb/s, 40 Gb/s, and above.

In order to use a fiber link with PMD to carry optical signals at ever increasing data rates without channel degradation, compensation for PMD is necessary. While several PMD compensation approaches have been reported [4]–[6], only those that fully compensate PMD in a link by tracking variations in the DGD and PSP's are viable. The approach presented here attempts to compensate fully for the effects of PMD on a single optical channel over a fiber link.

II. Active PMD Compensation

In the system we developed, the PMD adaptive compensation system treats the PMD on the link as a vector quantity, with DGD as the magnitude and PSP as the direction. A PMD component of equal magnitude but opposite in direction is applied to the signal in the receiver so that the vector sum results in zero PMD. To accomplish this, an accurate and reliable technique for monitoring the PSP's and the DGD of the fiber link was developed, together with a means of producing a complementary PMD vector in the receiver. A block diagram of our system, shown in Fig. 1, illustrates the elements of the adaptive PMD compensation system and shows the evolution of the envelope and state of polarization for a single transmitted pulse as it progresses from the transmitter through the link, after the polarization controller and as it emerges from the PMD emulator. The control parameters (θ_e, ϕ_e, and DGD$_e$) correspond to the settings for compensating the effects of PMD in the link.

To monitor the effect of PMD on the received signal, we adopted the method presented by Takahashi *et al.* [4]. The power level of a nonreturn-to-zero (NRZ) signal's spectral component corresponding to one-half of the data rate can serve as an indicator of PMD in a fiber link. For example, to monitor the PMD on a 10-Gb/s NRZ signal, the power of the spectral component at 5 GHz is monitored. Implementing this approach involves a narrowband bandpass filter centered at 5 GHz followed by a square-law detector and a low-pass filter. The output signal is maximized when the PMD affecting the optical NRZ signal is minimized. The shape of the transfer function relating PMD (more specifically, DGD) to the level of this *monitor signal* is approximately quadratic (as shown in Fig. 3).

The compensating PMD introduced in the receiver is set by a polarization controller and a PMD emulator. The polarization controller rotates the link's output PSP's to align with the input PSP's of the PMD emulator (which turn out to be linearly polarized). The PMD emulator introduces the desired time delay (DGD) between two orthogonally polarized optical paths by splitting the input signal based on its polarization and preferentially delaying one of the two paths before recombining the two orthogonally polarized signals. Through this approach, the two output pulses that result from PMD on the link are precisely superimposed in time, effectively undoing the effects of the link's PMD.

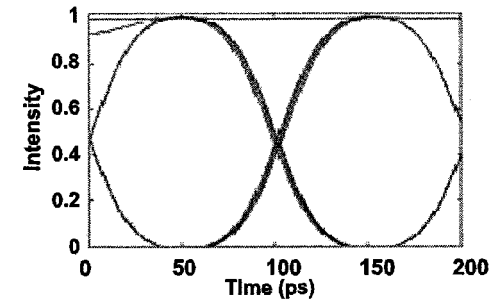

(a)

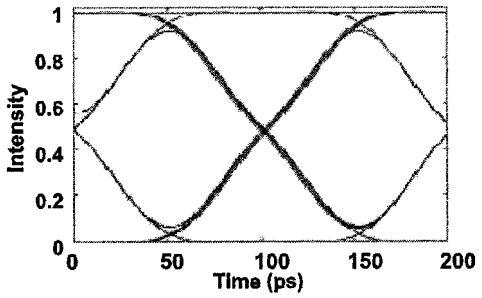

(b)

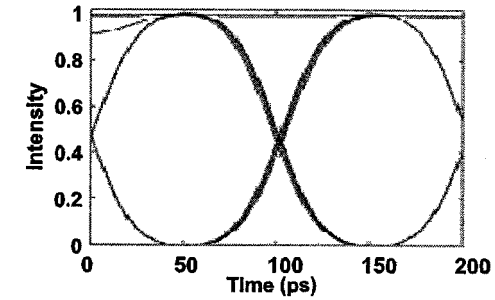

(c)

Fig. 4. Eye diagrams at different locations along the link in a simulated 10-Gb/s NRZ system: (a) transmitter output, (b) optical link output, and (c) PMD compensation system output. Assumes equal power on the link's input PSP's and 50 ps of DGD in the link. The adaptive PMD compensation system is set to compensate fully for the effects of PMD in the link.

III. Computer Simulation

Computer simulations were conducted to determine the effectiveness of this approach. In the simulation, a 10-Gb/s NRZ signal having a known SOP was launched into a fiber link having a selectable PMD (PSP's and DGD). At the receiver, the signal was passed through our PMD compensation system and the power of the 5-GHz spectral component (the monitor signal) was determined. The polarization controller was modeled as a combination of two quarter-wave plates (QWP's) and a half-wave plate (HWP), arranged as QWP-HWP-QWP. For this arrangement, the polarization controller can be simulated using a transformation matrix associated with only two free parameters, the phase angle of the HWP and that of the first QWP, since the phase angle of the first QWP and that of the last QWP are always180° apart.

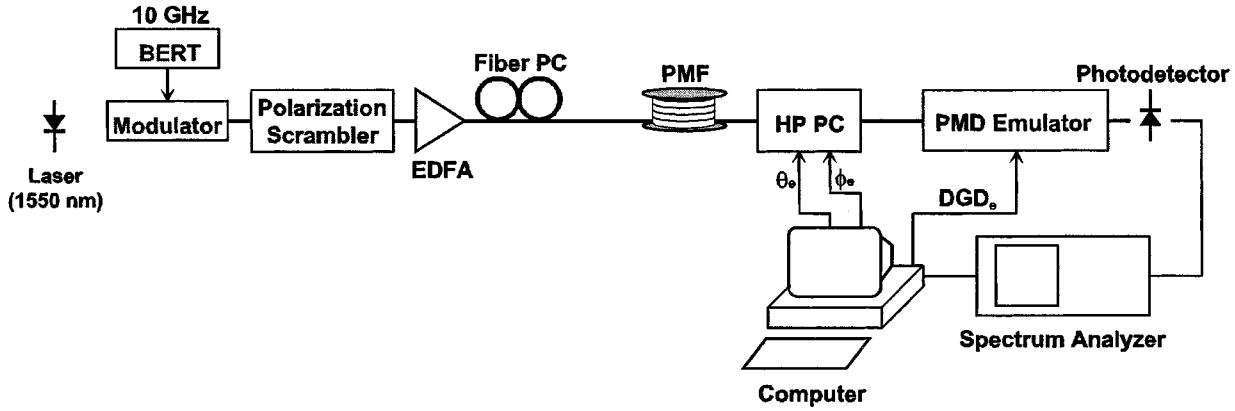

Fig. 5. Experimental setup for evaluation of the adaptive PMD compensation system. EDFA: Erbium-doped fiber-optic amplifier; fiber PC: fiber polarization controller; PMF: polarization-maintaining fiber; HP PC: HP polarization controller.

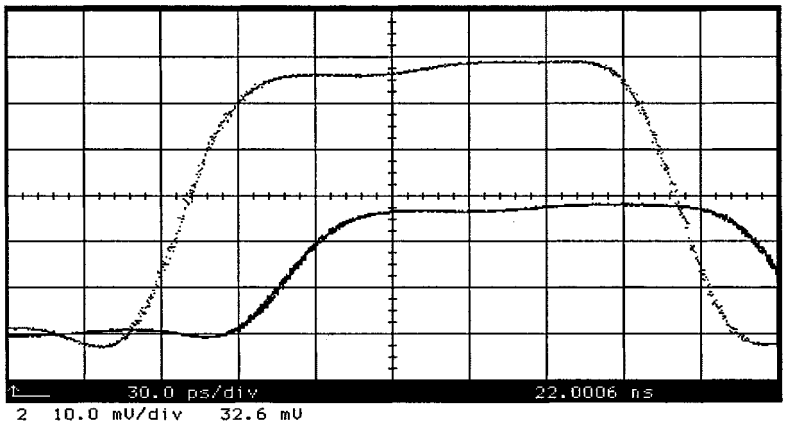

Fig. 6. Timing relationship of two orthogonal pulses obtained from the output of the PMD emulator showing the induced DGD of 48 ps. The different pulse levels of the signal traces indicate an unequal power splitting (approximately 70/30) between the emulator's PSP's.

To examine how the monitor signal power varies with polarization controller setting, we assumed a priori knowledge of the link's DGD (50 ps in this case) and set the emulator's DGD to correspond. The monitor signal power was determined for all possible settings of the polarization controller (with two degrees of freedom) to produce a surface. The coordinates of the peak of the surface correspond to the polarization controller settings that align the link's PSP's with the PSP's of the emulator. For the case where the input signal's SOP aligned such that its power is equally split between the link's PSP's, this procedure produces a surface with a single peak as shown in Fig. 2.

We next examined how the monitor signal varies with DGD in the PMD emulator. We began by setting the emulator's DGD to an arbitrary (but nonzero) value of 15 ps. In an effort to maximize the sensitivity of the monitor signal to DGD variations, we deliberately misaligned the PSP's of the link with those of the PMD emulator by setting the polarization controller such that the monitor signal is minimized. This approach is necessary to resolve small values of link DGD and to accommodate unequal power splitting between the PSP's. For example, in the case where the transmitter SOP is aligned with one of the link's input PSP's and consequently the link effectively exhibits no PMD, this polarization controller setting yields an unambiguous link DGD estimate of zero; otherwise variations in the PMD emulator DGD produces no change in monitor signal power.

We then varied the emulator's DGD and observed changes in the monitor signal level. Fig. 3 illustrates the transfer function relating emulator DGD and monitor signal level for the case where the link DGD was 10 ps and the input SOP was aligned such that its power is equally split between the link's PSP's. The resulting curve has the expected shape, with a maximum (representing a minimization in the overall PMD) when the emulator DGD exactly cancels the DGD in the link; that is, -10 ps.

To show the effectiveness of the simulated PMD compensation system, eye diagrams of a 10-Gb/s NRZ signal were produced for the signal at the transmitter, at the output of the fiber link (but prior to the PMD compensation system), and at the output of the PMD compensation system, as shown in Fig. 4. The eye-diagrams produced from the computer simulations include an 8-GHz, fifth-order low-pass Bessel filter used as a post-detection filter to suppress high frequency components. In the link, the DGD is 50 ps and the input SOP is oriented such that the power is equally split between the link's input PSP's. The eye at the output of the fiber link is clearly distorted, most notably by the reduced slope at the bit transitions, resulting in an eye closure penalty of 0.8 dB compared to the eye diagram

at the transmitter. Assuming a jitter window width of 10 ps centered on the eye opening, the eye-closure penalty is computed by comparing the vertical dimension of the eye opening with that of the eye measured at the transmitter. The difference between the eye diagram at the transmitter and that at the output of the PMD compensation system is negligible (0 dB eye-closure penalty), demonstrating the effectiveness of the compensation technique.

IV. Experimental Validation

Laboratory tests were conducted to validate the results of the computer simulation. Fig. 5 shows the block diagram of the laboratory test setup. A 10-Gb/s NRZ signal was produced with a bit-error rate tester (BERT) driving a Mach–Zehnder modulator to intensity modulate a 1550-nm continuous-wave (CW) optical signal followed by a lithium-niobate phase shifter that serves as the polarization scrambler. (The SOP input is deliberately aligned midway between the phase shifter's fast and slow axis so that an applied voltage results in a phase shift between the two propagating waves producing a change in the output SOP.) Next is an erbium-doped fiber amplifier (EDFA) to boost the signal level. A link DGD of 48 ps was created using 23 m of polarization maintaining fiber (PMF). To vary the power distribution between the two PSP's in the PMF when the polarization scrambler was not activated, a manually controlled (paddle-type) fiber polarization controller was placed immediately between the EDFA and the PMF. Fig. 6 shows the signal output from the PMF when a 200-ps-long pulse is launched with its SOP aligned relative to the PSP's to yield an unequal power split of approximately 70/30 in this case.

Orientation control of the receiver's PSP's relative to the PSP's of the PMF was achieved with an HP 11896A computer-controlled polarization controller. The polarization controller is followed by a computer-controlled PMD emulator to introduce the compensation DGD. In this device, the incoming optical signal is decomposed into its two orthogonal, linear polarization components, which propagate along separate optical paths that are ultimately recombined with their polarization states preserved. As the path length of one of the two paths is variable while the path length of the other is constant, various amounts of DGD can be produced, both positive and negative. The computer-controllable JDS PE3050 PMD emulator used in our experiments has a DGD range of -30 to $+125$ ps and a resolution of 0.002 ps.

The output of the PMD emulator is connected to a photodetector to convert the signal from the optical domain to the electronic domain. Following the photodetector is a 7.5-GHz LPF. The signal is then split, one portion going to a high-speed oscilloscope to monitor the signal's eye diagram, and the other portion sent to an HP 8592L microwave spectrum analyzer where the power of the 5-GHz spectral component (the monitor signal) was measured. The spectrum analyzer was configured to provide a digital output signal representing the bandlimited (300 kHz bandwidth) power of this spectral component. This monitor signal is then used by a computer to determine the control parameters for the polarization controller and the PMD emulator, through a sequential search process aimed at maximizing the monitor signal power.

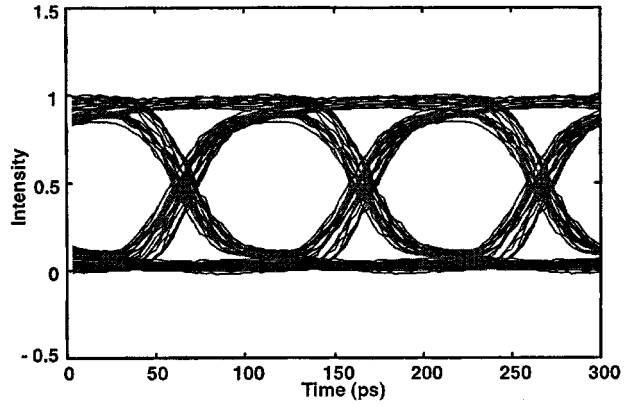

(a)

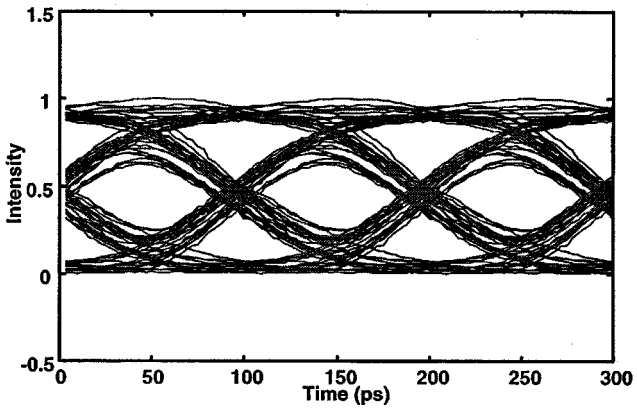

(b)

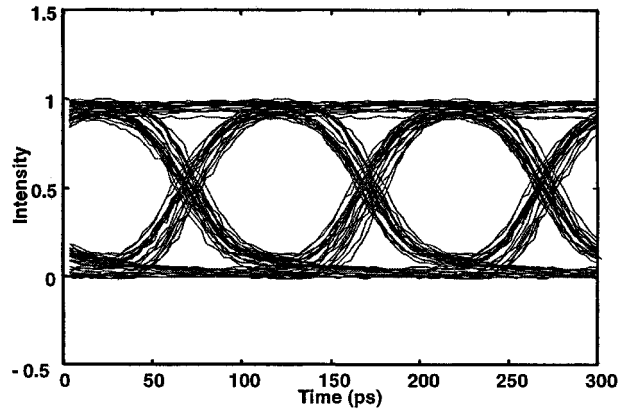

(c)

Fig. 7. Eye diagrams for a 10-Gb/s NRZ system with equal power distribution on the link's input PSP's and 48 ps of DGD in the link measured at different locations along the link: (a) transmitter output, (b) optical link output, and (c) PMD compensation system output.

Fig. 7 shows the eye diagram for the signal at various points in the system. First is the eye diagram of the signal output from the transmitter. Next is the eye diagram of the signal output from the PMF for equal power splitting between the PSP's. The most

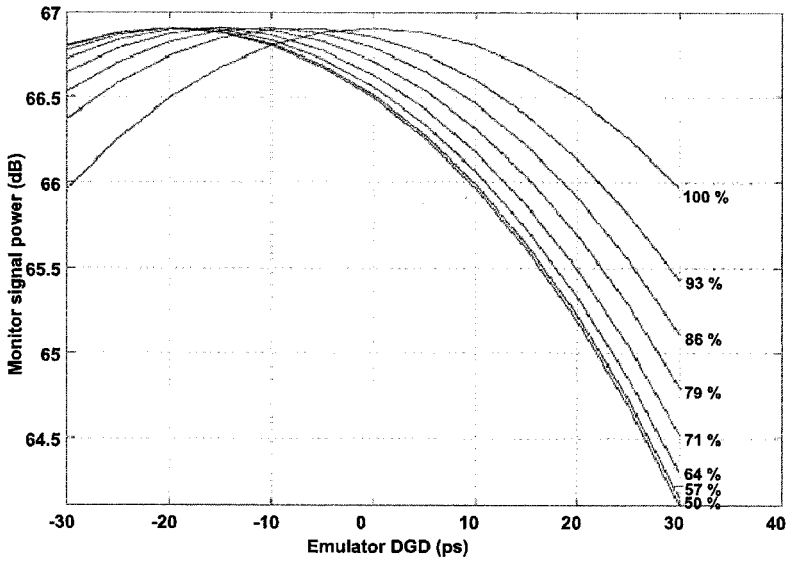

Fig. 8. Collection of curves representing the monitor signal power versus link DGD for various signal power distributions on the input PSP's. Power ratio at the input PSP's vary from 50/50 to 100/0 in increments of 7.14. The simulated link DGD is 20 ps.

notable effect of the 48 ps of DGD introduced by the PMF is the reduced slope at the bit transitions. Finally, we show the eye diagram of the signal output from the PMD compensation system, where the quality of the eye has been largely restored to its original shape. Using the transmitter output eye opening as a reference and a 10-ps jitter window width, the eye-closure penalty of the signal at the output of the PMF is 3.8 dB, while at the output of the PMD compensation system the eye-closure penalty is 0.07 dB. The difference in eye-closure penalties between the simulation and the laboratory measurements may be attributed to amplitude and phase ripple in the system transfer function (including the modulator, photodetector, electrical post-detection filter) in the hardware but not accounted for in the simulation.

V. SOP/PSP Alignment Effects

As mentioned above, the ability to monitor the state of the PSP's and DGD on a link reliably is somewhat dependent on the input SOP exciting both PSP modes in the link. Instances where the input SOP is nearly aligned with one of the link's input PSP's significantly degrades the ability of the monitoring system to track the PSP's and the DGD.

To investigate the effects of various SOP / PSP alignments, computer simulations of the PMD compensation system were conducted. As before, a 10-Gb/s NRZ signal having a known SOP is launched into a fiber link having a selectable PMD (PSP's and DGD). At the receiver, the signal is passed through the PMD compensation system and the power of the monitor signal is determined. Setting the polarization controller so that the link's PSP's and the PSP's of the PMD emulator are misaligned as before, we estimate the DGD in the link by varying the emulator's DGD and observe changes in the monitor signal level. With the link DGD set at 20 ps, Fig. 8 shows results for several cases representing various alignments of the input SOP with the link's input PSP's. For the case where the SOP is aligned such that the input power is nearly evenly split, the location of the maximum approximates the actual link DGD, i.e., 20 ps. However, as the splitting ratio becomes more and more unbalanced, the emulator DGD that maximizes the monitor signal power moves progressively toward zero. Finally the case where all of the power is launched along one PSP results in a curve that peaks at zero DGD in the emulator, despite the fact that the link's DGD is 20 ps. Hence the use of this parameter to estimate the link's DGD is sensitive to the relative alignment of the input signal's SOP and the link's input PSP's.

The relative alignment of SOP and PSP's also affects the transfer function relating the monitor signal power to the state of the polarization controller. To illustrate this, we again present computer simulations of the PMD compensation system as before. For this evaluation, we assume *a priori* knowledge of the link's DGD and set the emulator's DGD to correspond. The monitor signal power is determined for all possible settings of the polarization controller with two degrees of freedom to produce a surface plot. The coordinates of the peak of the surface corresponds to the polarization controller settings that align the link's PSP's with the PSP's of the emulator. For the case where the input signal's SOP is aligned such that its power is equally split between the link's PSP's, a surface with a single peak is produced as was shown previously in Fig. 3. However, as the alignment between the input SOP and the link's input PSP's is changed, the shape and nature of the surface changes also. In Fig. 9(a) the alignment producing a 70/30 distribution of the signal power on the PSP's results in a surface with two unequal peaks. In Fig. 9(b) the alignment is changed so that all of the signal power is coupled into a single PSP. In this case, two peaks of equal amplitude are observed, each corresponding to a case where 100% of the signal is routed through only one branch of the PMD emulator, as would be expected, and the two peaks represent two orthogonal polarization controller settings.

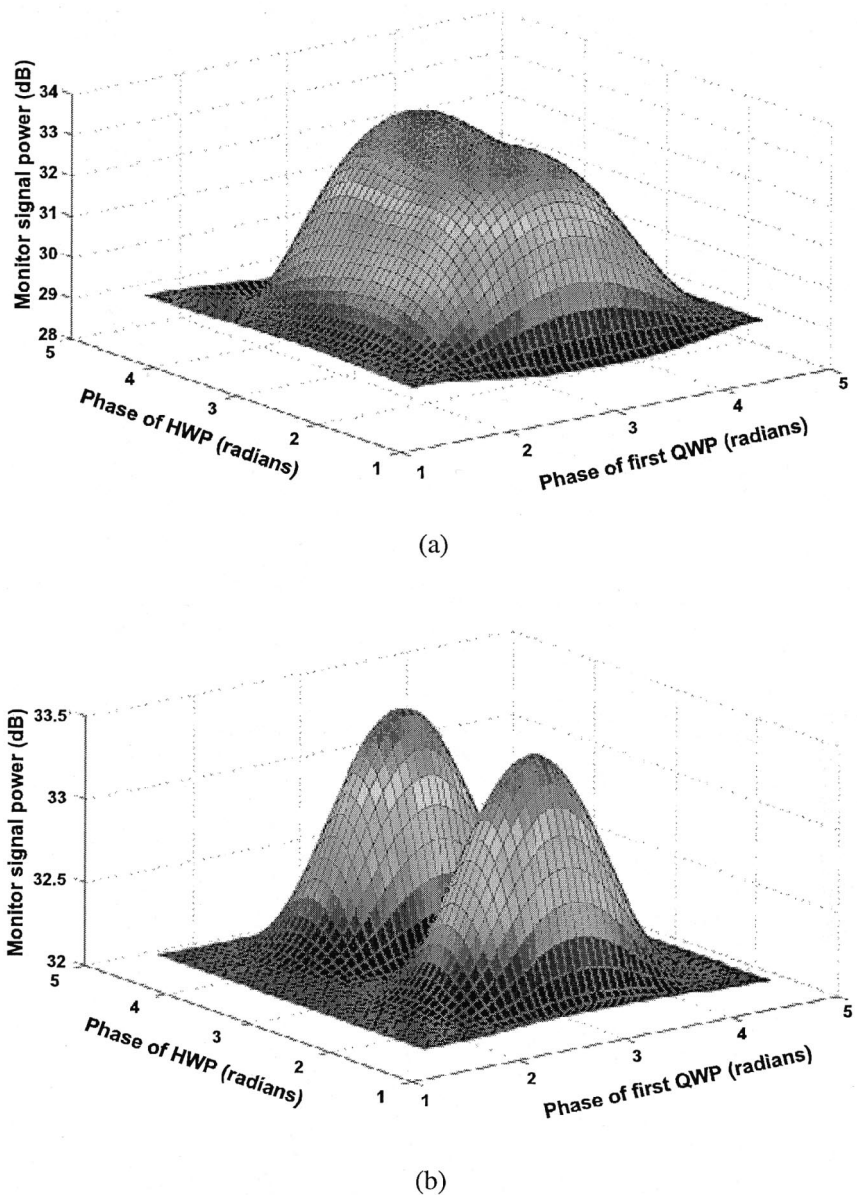

Fig. 9. Three-dimensional presentation of how the monitor signal varies with polarization controller setting with the input SOP fixed relative to the fiber PSP: (a) 70/30 signal power split onto the input PSP's and (b) all power is launched onto one of the input PSP's.

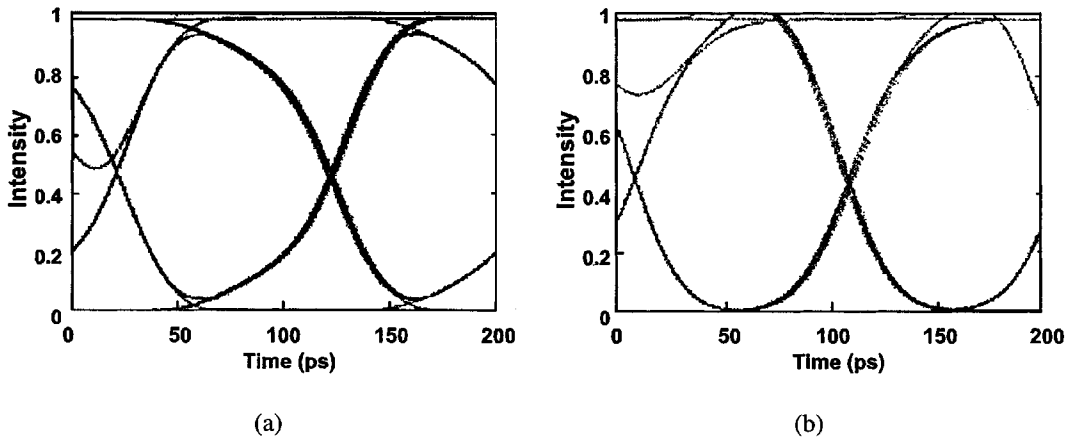

Fig. 10. Eye diagrams for a simulated 10-Gb/s NRZ system with a 70/30 power distribution on the link's input PSP's and 50 ps of DGD in the link measured at: (a) optical link output and (b) PMD compensation system output. The adaptive PMD compensation system is set to compensate fully for the effects of PMD in the link and there is no polarization scrambling at the transmitter.

VI. Polarization Scrambling

Based on these results, it is clear that the use of the monitor signal alone to determine the proper PMD compensation system settings is inadequate; knowledge of the relative alignment between the input signal's SOP and the link's input PSP's is also needed. Since the link's input PSP's are time varying, tracking with the launched signal's SOP orientation is not possible without additional information. To overcome this challenge, we scrambled the SOP of the input signal at the output of the transmitter. While the relative alignment between the SOP and the link's input PSP's is still not known at any instant, we do know that over a given interval determined by the frequency of the polarization scrambler a variety of relative alignments is realized. Additionally, for truly random SOP scrambling, the alignment having the greatest probability is where the power is equally split, and the lowest probability is where all of the power propagates along a single PSP. Therefore the estimate of the proper settings for the PMD compensation system based on the monitor signal is greatly improved when the input SOP is scrambled.

Simulation results confirm the effectiveness of this approach. When the input signal's SOP is scrambled at a rate much greater than the response time of the lowpass filter and each sample represents multiple alignments, the estimate of the compensating DGD and polarization controller setting agrees with the estimates obtained when the input SOP is static and aligned such that the power is evenly split between the PSP's. Fig. 10 shows the simulated eye diagrams for the case of an unequal power split (70/30) without polarization scrambling. The eye diagram shown in Fig. 10(a) represents the signal at the link output, prior to the PMD compensation system. The eye-closure penalty compared to the transmitted signal as shown in Fig. 4 is 0.5 dB. Fig. 10(b) shows the eye diagram of the signal output from the PMD compensation system that has been configured to maximize the monitor signal power. While the PMD compensation system has improved the signal, some distortion of the eye remains and the eye closure penalty is 0.25 dB. When polarization scrambling is present, the eye diagram at the PMD compensation system is identical to that shown in Fig. 4(c), with a negligible eye-closure penalty.

Experimental results also demonstrate that polarization scrambling improves the effectiveness of the PMD compensation system. The experimental setup described previously was configured to produce an SOP alignment that resulted in a power split of approximately 70/30 between the PSP's in the PMF. The eye diagram at the output of the PMF is shown in Fig. 11(a) and has an eye-closure penalty of 2.5 dB compared to the transmitted eye. The eye diagram at the output of the PMD compensation system configured to maximize the monitor signal is shown in Fig. 11(b). While the resultant eye diagram is improved compared to the uncompensated eye, the eye-closure penalty is 0.79 dB. Finally, the eye diagram shown in Fig. 11(c) represents the case where the polarization scrambler at the output of the transmitter is activated and the PMD compensation system again determines the appropriate settings that result in a maximum monitor signal power. The eye closure penalty for this eye diagram is 0.15 dB. Hence in this case, polarization scrambling improves our ability to compensate for PMD by more than 0.6 dB.

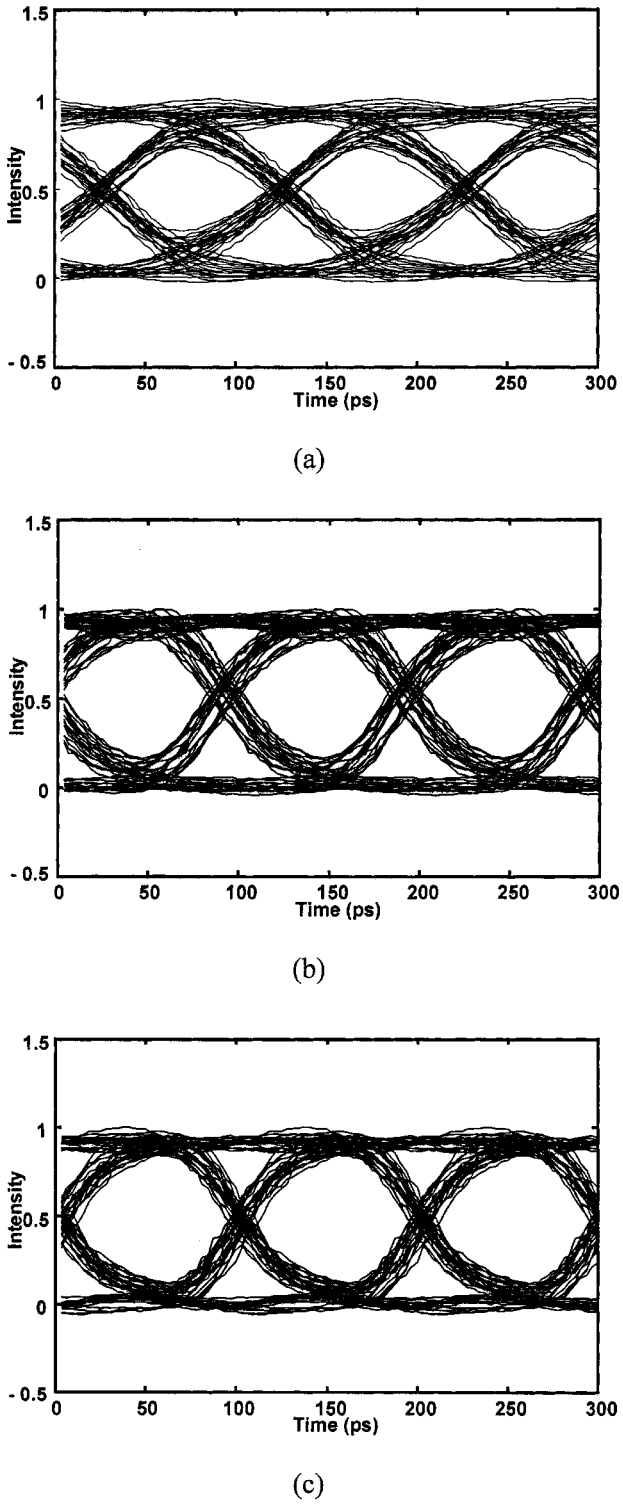

Fig. 11. Eye diagrams of the signal received from a link having 48 ps of DGD and a 70/30 power split: (a) before the PMD compensation system, (b) after the PMD compensation system without polarization scrambling, and (c) after the PMD compensation system with polarization scrambling.

In this experiment, the polarization scrambler was driven by a sinusoidal voltage with an amplitude sufficient to produce an

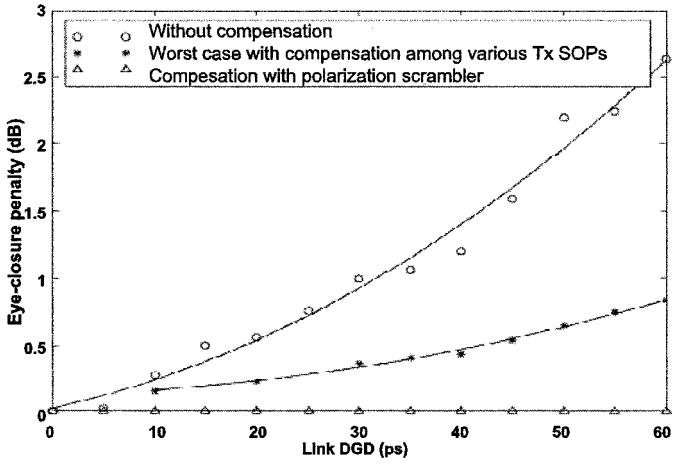

Fig. 12. Overview of signal eye-pattern degradation due to PMD effects for various degrees of PMD compensation.

orthogonal polarization. When viewed on the Poincare sphere, the resulting SOP's would ideally map out a great circle. While an ideal polarization scrambler would result in a uniform SOP distribution on the Poincare sphere, this approach sufficiently weights monitor signal with samples where the SOP is equally split between the PSP's so as to improve the DGD estimate. The frequency of this signal was approximately 1 GHz in this experiment.

To summarize the effectiveness of the PMD compensation system both with and without the benefit of a polarization scrambler at the transmitter, Fig. 12 presents the eye-closure penalty for various fiber DGD cases for a simulated 10-Gb/s NRZ signal. Three compensation modes are presented: no compensation system; compensation system active but no SOP scrambling; and active compensation with SOP scrambling. Symbols denote particular simulation results and the curves represent a best-fit interpolation. For the case of no compensation and variable power splitting between the PSP's, the eye degradation increases monotonically with increasing link DGD. For the case of active compensation without SOP scrambling, the eye degradation is substantially improved; however the degradation is not eliminated. For the case of active compensation with SOP scrambling, the eye degradation due to PMD is essentially eliminated.

VII. Conclusion

An adaptive PMD compensation system has been developed that cancels the effects of first-order PMD by producing a complementary PMD vector in the receiver. Control parameters for the PMD compensation system comprised of a polarization controller and a PMD emulator are derived from the NRZ signal in the channel to be compensated. Estimates of the link's DGD and PSP's based on this signal are reliable when the signal power is equally split between the link's two PSP's; however, this condition cannot be assumed. To meet this requirement, we scramble the SOP of the input signal at a rate much greater than the response time of the PMD monitor signal so that each sample represents many different SOP alignments. This approach allows the effective cancellation of the PMD effects within an optical fiber channel. As this approach relies on the PSP concept, this compensation technique addresses only first-order PMD; consequently in a wavelength-division multiplexing (WDM) application, a separate PMD compensation system would be required for each optical channel.

References

[1] E. Iannone, F. Matera, A. Mecozzi, and M. Settembre, *Nonlinear Optical Communication Networks*. New York: Wiley, 1998, pp. 30–35.
[2] C. D. Poole and J. Nagel, "Polarization effects in lightwave systems," in *Optical Fiber Telecommunications III A*, I. P. Kaminov and T. L. Koch, Eds. San Diego, CA: Academic, 1997.
[3] S. Betti, F. Curti, B. Daino, G. De Marchis, E. Iannone, and F. Matera, "Evolution of the bandwidth of the principal states of polarization in single-mode fibers," *Opt. Lett.*, vol. 16, no. 7, pp. 467–469, 1991.
[4] T. Takahashi, T. Imai, and M. Aiki, "Automatic compensation technique for timewise fluctuating polarization mode dispersion in in-line amplifier systems," *Electron. Lett.*, vol. 30, pp. 348–349, 1994.
[5] F. Heismann, D. A. Fishman, and D. L. Wilson, "Automatic compensation of first-order polarization mode dispersion in a 10-Gb/s transmission system," in *Proc. ECOC'98*, vol. I, Madrid, Spain, 1998, pp. 529–530.
[6] Z. Haas, C. D. Poole, M. A. Santoro, and J. H. Winters, "Fiber-optic transmission polarization-dependent distortion compensation," U.S. Patent 5 311 346, 1994.

Hok Yong Pua, photograph and biography not available at the time of publication.

Kumar Peddanarappagari, photograph and biography not available at the time of publication.

Benyuan Zhu, photograph and biography not available at the time of publication.

Christopher Allen (M"94——SM"95) was born in Independence, MO, on October 7, 1958. He received the B.S., M.S., and Ph.D. degrees in electrical engineering from The University of Kansas, Lawrence, in 1980, 1982, and 1984, respectively.

From 1984 to 1990, he was with Sandia National Laboratories, Albuquerque, NM, working in exploratory radar systems and development of high-speed digital systems. From 1990 to 1994, he was with the Allied Signal Kansas City Division, Kansas City, MO, where he worked in the areas of high-speed digital design, radar systems analysis, and multichip module development. Since August 1994, he has been a faculty member in the Electrical Engineering and Computer Science Department at The University of Kansas. His research interests include high-speed digital circuits, microwave remote sensing, radar systems, and photonics/lightwave technologies.

Dr. Allen has served as a technical reviewer for various IEEE journals and Remote Sensing of the Environment, Geophysics—, The Journal of the Society of Exploration Geophysicists, and Journal of Glaciology. He currently is the director of the Radar Systems and Remote Sensing Laboratory and co-Director of the Lightwave Communication Systems Laboratory. He also serves on the SAE AE-8D task group on standards development for Fiber Optic Cable and Test Methods for aerospace applications. He is a member of Phi Kappa Phi, Tau Beta Pi, Eta Kappa Nu, and the International Union of Radio Science (URSI).

Kenneth Demarest, photograph and biography not available at the time of publication.

Rongqing Hui received the B.S. degree in microwave communications and the M.S. degree in lightwave technology from Beijing University of Posts & Telecommunications, Beijing, China, in 1982 and 1988, respectively. He received the Ph.D degree in electrical engineering from Politecnico di Torino, Torino, Italy, in 1993.

From 1982 to 1985, he taught at the Physics Department of Anhui University, Hefei, China, where he also conducted research on optical fibers and fiber sensors. From 1985 to 1989, he was with the Optical Communication Laboratory of Beijing University of Posts & Telecommunications, where he worked in coherent optical fiber communication systems and components. From 1989 to 1990, he held a research fellowship from the Fundazione Ugo Bordoni, Rome, Italy, working on nonlinear effects and optical injection locking of semiconductor laser devices. From 1990 to 1993, he was with the Department of Electronics, Politecnico di Torino, where he worked on optical communications and single frequency semiconductor laser devices. During this period, he also held a fellowship from the Italian Telecommunication research Center (CSELT), Torino, Italy, where his research subject was polarization-insensitive coherent optical communication systems. From 1993 to 1994, he was a Postdoctoral Research Fellow working on optical systems and networks architecture at the University of Ottawa, Ont., Canada. He joined Bell-Northern Research (now part of Nortel), Ottawa, Ont., Canada, in 1994 as a Member of Scientific Staff, where he has worked in the research and development of high-speed optical transport networks. Since September 1997, he has been a faculty member in the Electrical Engineering and Computer Science Department, The University of Kansas. As an author or coauthor, he has published more than 60 journal and conference papers and holds a number of patents. He also acted as a technical reviewer for various IEEE, IEE, and OSA journals.